ROYAL SOCIETY OF CHEMISTRY

PAPER

Conventional Type II photoinitiators as activators for photoinduced metal-free atom transfer radical polymerization

Andrit Allushi, Ceren Kutahya, Cansu Aydogan, Johannes Kreutzer,* Gorkem Yilmaz* and Yusuf Yagci*

A novel methodology for photoinduced metal-free Atom Transfer Radical Polymerization (ATRP) by using conventional Type II photoinitiators such as benzophenone, thioxanthone, isopropyl thioxanthone and camphorquinone as sensitizers is presented. These sensitizers efficiently activate the ATRP of vinyl monomers when used in conjunction with co-initiators and alkyl halides under light irradiation. DFT calculations were performed to reveal mechanistic aspects and showed that the initiation of the controlled ATRP reaction pathway from the triplet state is energetically favoured for all sensitizers. In the case of benzophenone, however, the hydrogen abstraction pathway, which leads to free radical polymerization, is a possible side reaction. The strategy applied was proved to yield polymers with narrow molecular distribution. The chain-end fidelity of the polymer obtained was approved by chain extension and block copolymerization experiments, whereas the irradiation dependency of polymerization was confirmed by light on/off experiments.

Introduction

Photoinitiators are the most important elements of photopolymerization processes as they are responsible for the transformation of light energy to chemical energy.[1] Among the various modes of photopolymerization,[2–6] free radical polymerization is in a more advanced state due to the wavelength flexibility and broad availability of monomer formulations. Free radical photoinitiators are divided into two classes depending on their decomposition mechanism. Type I or α-cleavage photoinitiators undergo decomposition directly after irradiation to yield radicals that can initiate polymerization. Type II photoinitiators generate radicals in the presence of co-initiators in a multi-step reaction mechanism. If an amine is used as a co-initiator, generally an electron is transferred to the triplet state of the Type II initiator, followed by a proton release to generate radicals.[7] Typical examples of commercially available Type II initiators include benzophenone (BP), thioxanthone (TX) and their derivatives, and camphorquinone (CQ), which have a broad wavelength absorption in the UV-vis range of the electromagnetic spectrum. Among them, TXs are the most widely used photoinitiators due to their absorption characteristics and high quantum efficiency.[7] These photo-

initiators are often employed for free radical[8–16] and cationic polymerization[17] and as catalysts for photoinduced click reactions[18,19] and also as anticancer agents.[20] Scheme 1 shows the initiation of the radical polymerization process with TX as an example. Notably, ketyl radicals formed on the photoinitiator skeleton do not initiate polymerization due to resonance stability and steric effects, whereas radicals from the co-initiator are responsible for the initiation.

Besides such applications, these photoinitiators were also applied in atom transfer radical polymerization (ATRP), start-
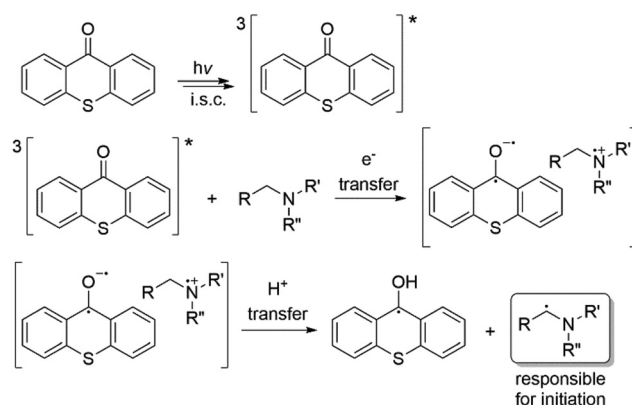
Scheme 1 Photoinitiated radical formation in a thioxanthone/amine system.

Department of Chemistry, Istanbul Technical University, 34469 Maslak, Istanbul, Turkey. E-mail: yusuf@itu.edu.tr, a.gorkemyilmaz@gmail.com, johannes.kreutzer@yahoo.com

ing from high oxidation state copper halides.[21] In conventional ATRP, Cu(I) halides together with a suitable ligand system and an alkyl halide are used as redox active species.[22] The air sensitivity of these metal catalysts and limitations concerning the bio-applications of the obtained polymers led to the development of approaches to generate Cu(I) *in situ* and where ppm levels of Cu catalysts are sufficient to initiate the polymerization. Reported strategies include chemical,[23,24] electrochemical,[25] and photochemical reduction of Cu(II) species[26–28] in the polymerization system. Recent work concentrated on the *in situ* generation of Cu(I) catalyst by direct[29] and indirect photoinduced electron transfer processes utilizing photoinitiators,[30,31] sensitizers,[32] nanoparticles[33] and fullerene derivatives.[34] More recently, certain photosensitizers (PS) such as phenothiazine derivatives,[35,36] perylene,[37] pyrene[38] and diaryl-dihydrophenazines[39] were found to realize photoinduced ATRP even in the absence of copper catalysts through an oxidative quenching pathway. In the proposed mechanism, an alkyl halide is reduced by photoinduced electron transfer from the excited state to generate radicals capable of initiating polymerization and the control over polymerization is achieved by the reversibility of activation/deactivation steps as depicted in Scheme 2.

Similar photo-redox reactions were also proposed for reducible dyes.[40,41] It seemed, therefore, appropriate to investigate whether Type II photoinitiators would act as activators for metal-free photo ATRP. Theoretical studies were performed to confirm the validity of the proposed mechanism.

As part of our continuous interest in developing photochemical systems for both conventional and controlled/living polymerization processes, we now report the application of commercially available Type II photoinitiators having different absorption characteristics and excited state properties for photoinduced metal-free ATRP. For this purpose, TX, BP, isopropyl thioxanthone (ITX) and CQ were used as PSs together with N,N,N',N'',N''-pentamethyldiethylenetriamine (PMDETA) and alkyl halides as the electron donor source and initiator, respectively, for the polymerization of various monomers.

PS: Photosensitizer

Scheme 2 Mechanism of photoinduced metal-free ATRP using PSs.

Experimental part

Materials

Thioxanthone (TX, 98%, Sigma Aldrich) was crystallized from ethanol prior to use. 2-Isopropylthioxanthone (ITX, Ward Blenkinsop and Co. Ltd), benzophenone (BP, 98%, Sigma Aldrich), and camphorquinone (CQ, 97%, Sigma Aldrich) were used as received. N,N-Dimethylformamide (DMF, EMPARTA, HPLC grade) was stored over activated molecular sieves (4 Å). N,N,N',N'',N''-Pentamethyldiethylenetriamine (PMDETA; Aldrich, 99%) was distilled before use. Ethyl α-bromoisobutyrate (EBI, 98%, Sigma Aldrich), ethyl 2-bromopropionate (EBP, 99%, Sigma Aldrich), and (1-bromoethyl)benzene (BEB, 97%, Sigma Aldrich) were used as received. Methyl methacrylate (MMA, 99%, Sigma Aldrich) and butyl acrylate (BA, 99.9%, Sigma Aldrich) were passed through basic alumina and stored under a nitrogen atmosphere in cold before use.

Instrumentation

^{1}H NMR spectra of the intermediates and final polymers were recorded at room temperature at 500 MHz on an Agilent VNMRS 500 spectrometer. UV spectra were recorded on a Shimadzu UV-1601 spectrometer. The resolution was 4 cm^{-1} and 24 scans were performed with a 0.2 cm s^{-1} scan speed. Gel permeation chromatography (GPC) measurements were performed from a Viscotek GPCmax autosampler system consisting of a pump, a Viscotek UV detector, and a Viscotek differential refractive index (RI) detector. Three ViscoGEL GPC columns (G2000H HR, G3000H HR, and G4000H HR, 7.8 mm internal diameter, 300 mm length) were used in series. THF was used as an eluent at a flow rate of 1.0 mL min^{-1} at 30 °C. Both detectors were calibrated with polystyrene standards having narrow-molecular-weight distribution. Data were analyzed using Viscotek OmniSEC Omni-01 software.

Calculations

All calculations were performed with the Gaussian09 program package.[42] Geometries were optimized with the B3LYP functional[43–45] in combination with the 6-31G(d) basis set. Dimer structures were optimized with the long range corrected CAM-B3LYP functional[46] in combination with the 6-31G(d) basis set. All geometries were confirmed as minimum structures displaying all frequencies real. Single point calculations were performed with the M06-2X functional and the 6-311++G (3df,2p) basis set. The combination of the M06-2X functional[47] and 6-311++G(3df,2p) basis set showed good performance for calculations of reaction enthalpies and reaction rates for electron transfer processes before.[48] The optimized structures, as well as single point energies were calculated with the Solvation Model based on Density (SMD) in DMF. Gibbs free energies and enthalpies include thermal corrections at 298 K.

General procedure for visible light induced metal-free ATRP of MMA

In a typical experiment, MMA (1 mL, 200 eq.), alkyl halide (1 eq.), DMF (1 mL), PMDETA (5 eq.) and photosensitizer

(TX, BP, ITX or CQ, 1 eq.) were put into a Schlenk tube and the reaction mixture was degassed by freeze–pump–thaw cycles and left in a vacuum ($\sim 10^{-3}$ bar). The stirring solution was irradiated with a light source emitting light nominally at 350 nm with a light intensity of 3.0 mW cm^{-2} for 4 h (in the case of CQ, the reaction mixture was irradiated at 400–500 nm with a light intensity of 45 mW cm^{-2}). At the end of the irradiation, the resulted polymers were precipitated in methanol and then dried under reduced pressure. Conversions were determined gravimetrically.

Results and discussion

TXs, BP and CQ as typical Type II photoinitiators appeared to be suitable candidates for UV-vis induced electron transfer processes because of their broad absorption spectra, covering the UV and visible spectral region and high molar absorptivities (Fig. 1). Initially, we examined the use of TX and BP as PSs for the polymerization of methyl methacrylate (MMA) in the presence of PMDETA and various alkyl halide sources, namely ethyl α-bromoisobutyrate (EBI), ethyl 2-bromopropionate (EBP) and (1-bromoethyl)benzene (BEB) as initiators at *ca.* 350 nm. As can be seen in Table 1 all yield polymers with low dispersities (<1.5), although at different conversions.

Apparently, with both sensitizers, longer polymerization times lead to higher conversions. With TX, an increase in polymerization time yields polymers with lower PDI values, whereas in the case of BP, a similar trend was not observed. This can be explained by the participation of two different polymerization mechanisms as discussed below (*vide infra*) (Table 2).

We then extended our experiments to other long wavelength absorbing PSs, namely ITX and CQ. Notably, higher conversions in the case of ITX indicate that this PS activates the polymerization more efficiently than the others do. In accordance with the absorption characteristics, the polymerization

Fig. 1 UV-vis spectra of thioxanthone, benzophenone, isopropyl thioxanthone and camphorquinone in DMF.

Table 1 Photo-induced metal-free ATRP[a] of MMA using TX and BP with different alkyl halides

Sensitizer	Initiator	Conv.[b] (%)	M_n[c] (g mol^{-1})	M_w/M_n[c]
TX	EBI	14.3	8900	1.38
BP	EBI	21.2	4750	1.42
TX	BEB	7.6	14 500	1.43
BP	BEB	8.1	11 700	1.34
TX	EBP	13.4	15 000	1.45
BP	EBP	1.7	12 300	1.50

[a] V_{MMA} = 1 mL, V_{DMF} = 1 mL, [MMA]/[RX]/[PMDETA]/[S]: 200/1/5/1, λ = 350 nm, time = 4 h. [b] Determined gravimetrically. [c] Determined by gel permeation chromatography using polystyrene standards.

Table 2 Effects of time on photo-induced metal-free ATRP[a] of MMA using EBI

Sensitizer	Time (h)	Conv.[b] (%)	M_n[c] (g mol^{-1})	M_w/M_n[c]
TX	4	14.3	8900	1.38
TX	8	24.5	15 100	1.33
TX	12	32.5	17 000	1.28
BP	4	21.2	4750	1.42
BP	8	47.0	6500	1.55
BP	12	57.3	9200	1.53

[a] V_{MMA} = 1 mL, V_{DMF} = 1 mL, [MMA]/[RX]/[PMDETA]/[S]: 200/1/5/1, λ = 350 nm, time = 4 h. [b] Determined gravimetrically. [c] Determined by gel permeation chromatography using polystyrene standards.

can be applied under visible light irradiation when CQ is used as a sensitizer (Table 3).

In addition, we were interested in the effect of the solvent on the polymerization and the results are depicted in Table 4. Expectedly, polymerizations in more polar solvents give higher
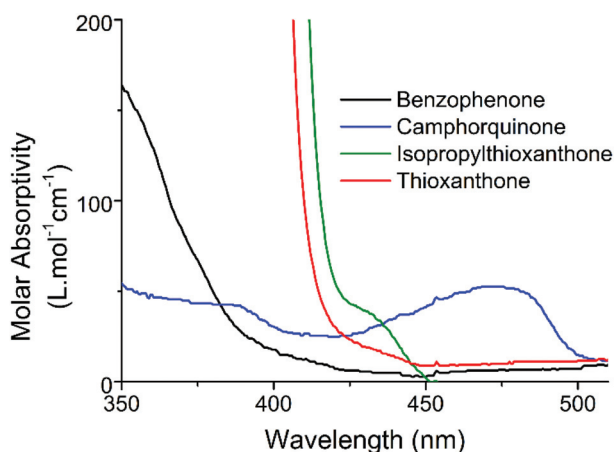
Table 3 Effects of sensitizer on photo-induced metal-free ATRP[a] of MMA using EBI

Sensitizer	Irradiation wavelength (nm)	Conv.[b] (%)	M_n[c] (g mol^{-1})	M_w/M_n[c]
ITX	350	59.0	11 200	1.74
CQ	400–500	17.0	8700	1.56

[a] V_{MMA} = 1 mL, V_{DMF} = 1 mL, [MMA]/[RX]/[PMDETA]/[S]: 200/1/5/1, time = 4 h. [b] Determined gravimetrically. [c] Determined by gel permeation chromatography using polystyrene standards.

Table 4 Effects of solvent on photo-induced metal-free ATRP[a] of MMA using ITX and EBI

Solvent	Polarity index	Conv.[b] (%)	M_n[c] (g mol^{-1})	M_w/M_n[c]
ACN	5.8	35.2	10 700	1.97
DMF	6.4	59.0	11 200	1.74
DMSO	7.2	65.8	12 500	1.56

[a] V_{MMA} = 1 mL, $V_{solvent}$ = 1 mL, [MMA]/[RX]/[PMDETA]/[ITX]: 200/1/5/1, λ = 350 nm, time = 4 h. [b] Determined gravimetrically. [c] Determined by gel permeation chromatography using polystyrene standards.

conversions and polymers with narrower dispersities further confirming involvement of electron transfer reactions and the ionic nature of the process. The ionic intermediates formed in the course of metal-free photo ATRP can be more easily stabilized in polar solvents.

In order to examine the chain-end fidelity of the polymers obtained, chain extension and block copolymerization experiments were performed. For this purpose, bromide chain-end functional PMMAs, which were obtained by the aforementioned process, were used as the halide source and identical polymerization conditions were applied as described in Table 1. In the chain extension process, MMA was used as a monomer, whereas for block copolymer synthesis, styrene was applied as a monomer. GPC analyses showed that there are clear shifts to lower retention volumes, which indicates the success of the polymerizations from the chain ends of the precursor PMMA in either case (Fig. 2).

Light on/off experiments were performed under identical experimental conditions as indicated in Table 3 at multiple quantities to test the dark reaction behavior. The polymerization mixture was placed in a Schlenk tube under a nitrogen atmosphere and subjected to repeated cycles of light exposure

(λ = 350 nm, 1 h illumination followed by a dark time of 30 min respectively). At the end of each step, equivalent volumes of the solution were precipitated into excess methanol to gravimetrically determine the conversion. The results demonstrate that the polymerization is irradiation dependent, and almost no polymerization occurred when the solutions were kept in the dark (Fig. 3). The minor increase in the conversion during the "dark" periods may be attributed to the slow deactivation rates of the propagating chains.

In the light of these studies and the general photoexcited state behavior of these sensitizers, the following mechanism can be proposed for the polymerizations on the example of TX (Scheme 3). The excited state of TX undergoes an electron transfer with electron donor amines. The formed radical anion form of TX reduces the initiator alkyl halide to yield radicals responsible for the initiation. A back electron transfer from the halide anion to the amine radical cation concludes the formation of the dormant macroalkyl halides that return to the polymerization cycle.

Mechanism

DFT calculations were performed to support the proposed mechanism. Reaction of the PSs under light irradiation and in the absence of the amine component PMDETA as well as the reaction without light irradiation did not occur. Thus, a direct electron transfer reaction between the sensitizer and the alkyl bromide, or an electron transfer reaction between the singlet ground state of the sensitizer (S_0) with either alkyl bromide or PMDETA can be disregarded. From this, it follows that in the reaction mechanism PMDETA must be first oxidized by an excited state of the PS. Upon excitation, the first excited singlet (S_1) or the triplet state (T) can theoretically be reduced to give the PS radical anion ($PS^{\circ-}$) and PMDETA radical cation ($PMDETA^{\circ+}$). Half reaction potentials of S_0, S_1 and T for the reduction of the PS were calculated and are summarized in Table 5. The oxidizing ability of the PS increases in the order $S_1 < S_0 < T$ which clearly indicates that the triplet state is the active species in the redox reaction with PMDETA.
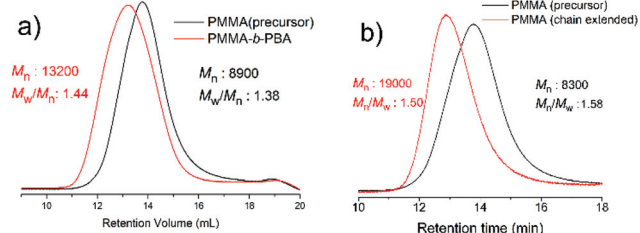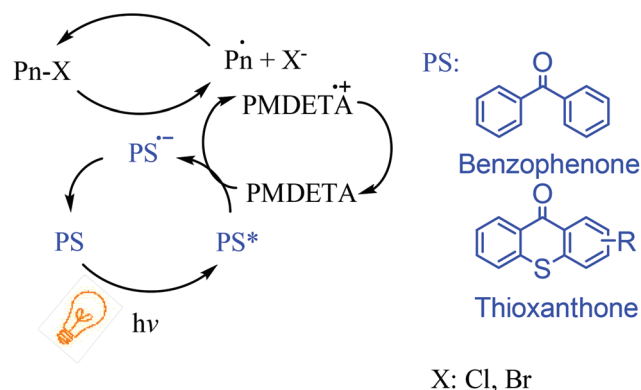

Fig. 2 Comparison of the GPC traces of precursor PMMA with (a) PMMA-*b*-PBA and (b) chain extended PMMA.

Fig. 3 Monomer conversion (%) *vs.* time using ITX to determine the dependency of propagation on irradiation: light on (yellow regions) light off (white regions).

Scheme 3 Proposed mechanism of photoinduced metal-free ATRP using the TX/amine initiating system.

Table 5 Half reaction potential ($E°$) of the photoinitiators calculated at the M06-2X|6-311++G(3df,2p) level of theory in DMF (SMD). Values are referenced to the standard hydrogen electrode (SHE)

Sensitizer	State	$E°$ vs. SHE [V]
ITX	S_0	−1.71
ITX	S_1	−1.86
ITX	T	1.22
BP	S_0	−1.64
BP	S_1	−1.85
BP	T	1.46
CQ	S_0	−1.51
CQ	S_1	−1.31
CQ	T	0.76

The reduced sensitizer can react either with EIB or with PMDETA to form an alkyl radical or a PMDETA radical which will eventually start the polymerization reaction (Scheme 4, reaction pathways II and III).

In the first case, PS$°^-$ undergoes hydrogen abstraction from PMDETA$°^+$ to give the protonated PS radical (PS-OH$°$) and a PMDETA radical (PMDETA$°$). In this pathway the PMDETA$°$ radical will initiate the polymerization and control over the polymerization reaction will be lost (see Scheme 4, pathway II). In the second case (Scheme 4, pathway III) PS$°^-$ reduces EIB to give the PS in its S_0 ground state, an alkyl radical and a bromine anion. Considering this reaction pathway, a controlled polymerization reaction according to ATRP is expected.

To gain more insight into the kinetics and thermodynamics of the possible pathways, Gibbs free energies and reaction enthalpies were calculated and are compared in Table 6.

Scheme 4 Possible pathways for the reaction mechanisms.

Table 6 Reaction enthalpies and Gibbs free energies of the different reaction pathways calculated at the M06-2X|6-311++G(3df,2p) level of theory in DMF (SMD)

Pathway	ΔH [kcal mol^{-1}]			ΔG [kcal mol^{-1}]		
	ITX	BP	CQ	ITX	BP	CQ
I	−11.82	−16.31	0.52	−11.15	−16.58	−0.68
II	−5.42	−13.03	−6.05	−6.56	−12.87	−5.97
III	−15.79	−15.77	−12.21	−15.02	−13.6	−10.42

The first step of the reaction, which is the reduction of the T state of the PS to give PS$°^-$ and PMDETA$°^+$, is thermodynamically favored for all three photoinitiators, with BP being the most favored followed by ITX and CQ. BP and CQ show negative reaction enthalpies, but not so CQ, which shows a slightly positive reaction enthalpy.

For all PS both possible consecutive reactions, the generation of the PMDETA radical (pathway II in Scheme 4) and the formation of the alkyl radical (pathway III in Scheme 4) are thermodynamically favored. Thus, free radical polymerization (reaction path II) as well as controlled ATRP (reaction path III) can potentially occur in a competing manner. However, the free energy and reaction enthalpy data suggest that reduction of the EIB compound will occur more likely than the proton transfer from PMDETA. In the case of BP the values are close to each other, which might make a potential contribution of the H-abstraction pathway possible with the consequence of loss over control of the polymerization reaction. This is well reflected in the higher PDI values of BP initiated polymerizations, when compared to e.g. ITX initiated polymerizations (see Table 2).

Conclusions

In conclusion, Type II photoinitiators were shown to activate metal-free ATRP under UV-vis light irradiation. The computational results give evidence that oxidation of the amine compound occurs from the triplet state of the PSs. In all cases the reaction kinetics for the controlled polymerization reaction are energetically favored. However, in the case of benzophenone, initiation of ATRP and free-radical polymerization pathway lie close to each other. Therefore, the free radical polymerization pathway cannot be excluded. Experimentally, this results in higher PDI values in comparison to TX. Light on/off experiments demonstrate the complete dependency of polymerization on irradiation, whereas chain extension and block copolymerization experiments approve the chain-end fidelity of the polymers obtained.

Acknowledgements

References

1 Y. Yagci, S. Jockusch and N. J. Turro, *Macromolecules*, 2010, **43**, 6245–6260.
2 J. P. Fouassier, X. Allonas and D. Burget, *Prog. Org. Coat.*, 2003, **47**, 16–36.

3 J. V. Crivello, *J. Polym. Sci., Part A: Polym. Chem.*, 1999, **37**, 4241–4254.

4 J. Lalevee, N. Blanchard, M. A. Tehfe, M. Peter, F. Morlet-Savary, D. Gigmes and J. P. Fouassier, *Polym. Chem.*, 2011, **2**, 1986–1991.

5 P. Xiao, J. Zhang, F. Dumur, M. A. Tehfe, F. Morlet-Savary, B. Graff, D. Gigmes, J. P. Fouassier and J. Lalevee, *Prog. Polym. Sci.*, 2015, **41**, 32–66.

6 J. P. Fouassier and J. Lalevee, *RSC Adv.*, 2012, **2**, 2621–2629.

7 J.-P. Fouassier, *Photoinitiation, photopolymerization, and photocuring: fundamentals and applications*, Munich; NewYork; Cincinnati, 1995.

8 M. Aydin, N. Arsu and Y. Yagci, *Macromol. Rapid Commun.*, 2003, **24**, 718–723.

9 D. K. Balta, N. Arsu, Y. Yagci, S. Jockusch and N. J. Turro, *Macromolecules*, 2007, **40**, 4138–4141.

10 L. Cokbaglan, N. Arsu, Y. Yagci, S. Jockusch and N. J. Turro, *Macromolecules*, 2003, **36**, 2649–2653.

11 G. Yilmaz, B. Aydogan, G. Temel, N. Arsu, N. Moszner and Y. Yagci, *Macromolecules*, 2010, **43**, 4520–4526.

12 D. Tunc and Y. Yagci, *Polym. Chem.*, 2011, **2**, 2557–2563.

13 G. Yilmaz, G. Acik and Y. Yagci, *Macromolecules*, 2012, **45**, 2219–2224.

14 G. Yilmaz, A. Tuzun and Y. Yagci, *J. Polym. Sci., Part A: Polym. Chem.*, 2010, **48**, 5120–5125.

15 S. Dadashi-Silab, C. Aydogan and Y. Yagci, *Polym. Chem.*, 2015, **6**, 6595–6615.

16 S. Kork, G. Yilmaz and Y. Yagci, *Macromol. Rapid Commun.*, 2015, **36**, 923–928.

17 G. Yilmaz, S. Beyazit and Y. Yagci, *J. Polym. Sci., Part A: Polym. Chem.*, 2011, **49**, 1591–1596.

18 M. Uygun, M. A. Tasdelen and Y. Yagci, *Macromol. Chem. Phys.*, 2010, **211**, 103–110.

19 S. Dadashi-Silab and Y. Yagci, *Tetrahedron Lett.*, 2015, **56**, 6440–6443.

20 G. Yilmaz, E. Guler, F. B. Barlas, S. Timur and Y. Yagci, *Macromol. Rapid Commun.*, 2016, **37**, 1046–1051.

21 O. S. Taskin, G. Yilmaz, M. A. Tasdelen and Y. Yagci, *Polym. Int.*, 2014, **63**, 902–907.

22 K. Matyjaszewski and J. H. Xia, *Chem. Rev.*, 2001, **101**, 2921–2990.

23 Y. Gnanou and G. Hizal, *J. Polym. Sci., Part A: Polym. Chem.*, 2004, **42**, 351–359.

24 K. Min, H. F. Gao and K. Matyjaszewski, *Macromolecules*, 2007, **40**, 1789–1791.

25 T. S. Hansen, J. U. Lind, A. E. Daugaard, S. Hvilsted, T. L. Andresen and N. B. Larsen, *Langmuir*, 2010, **26**, 16171–16177.

26 Z. B. Guan and B. Smart, *Macromolecules*, 2000, **33**, 6904–6906.

27 M. A. Tasdelen and Y. Yagci, *Angew. Chem., Int. Ed.*, 2013, **52**, 5930–5938.

28 M. A. Tasdelen, G. Yilmaz, B. Iskin and Y. Yagci, *Macromolecules*, 2012, **45**, 56–61.

29 M. A. Tasdelen, M. Uygun and Y. Yagci, *Macromol. Rapid Commun.*, 2011, **32**, 58–62.

30 M. Ciftci, M. A. Tasdelen and Y. Yagci, *Polym. Chem.*, 2014, **5**, 600–606.

31 M. A. Tasdelen, M. Uygun and Y. Yagci, *Macromol. Chem. Phys.*, 2011, **212**, 2036–2042.

32 M. A. Tasdelen, M. Ciftci and Y. Yagci, *Macromol. Chem. Phys.*, 2012, **213**, 1391–1396.

33 S. Dadashi-Silab, M. A. Tasdelen, A. M. Asiri, S. B. Khan and Y. Yagci, *Macromol. Rapid Commun.*, 2014, **35**, 454–459.

34 O. S. Taskin, G. Yilmaz and Y. Yagci, *ACS Macro Lett.*, 2016, **5**, 103–107.

35 N. J. Treat, H. Sprafke, J. W. Kramer, P. G. Clark, B. E. Barton, J. R. de Alaniz, B. P. Fors and C. J. Hawker, *J. Am. Chem. Soc.*, 2014, **136**, 16096–16101.

36 X. C. Pan, M. Lamson, J. J. Yan and K. Matyjaszewski, *ACS Macro Lett.*, 2015, **4**, 192–196.

37 G. M. Miyake and J. C. Theriot, *Macromolecules*, 2014, **47**, 8255–8261.

38 A. Allushi, S. Jockusch, G. Yilmaz and Y. Yagci, *Macromolecules*, 2016, **49**, 7785–7792.

39 J. C. Theriot, C. H. Lim, H. Yang, M. D. Ryan, C. B. Musgrave and G. M. Miyake, *Science*, 2016, **352**, 1082–1086.

40 C. Kutahya, F. S. Aykac, G. Yilmaz and Y. Yagci, *Polym. Chem.*, 2016, **7**, 6094–6098.

41 X. D. Liu, L. F. Zhang, Z. P. Cheng and X. L. Zhu, *Polym. Chem.*, 2016, **7**, 689–700.

42 M. J. Frisch, G. W. Trucks, H. B. Schlegel, G. E. Scuseria, M. A. Robb, J. R. Cheeseman, G. Scalmani, V. Barone, B. Mennucci, G. A. Petersson, H. Nakatsuji, M. Caricato, X. Li, H. P. Hratchian, A. F. Izmaylov, J. Bloino, G. Zheng, J. L. Sonnenberg, M. Hada, M. Ehara, K. Toyota, R. Fukuda, J. Hasegawa, M. Ishida, T. Nakajima, Y. Honda, O. Kitao, H. Nakai, T. Vreven, J. A. Montgomery Jr., J. E. Peralta, F. Ogliaro, M. J. Bearpark, J. Heyd, E. N. Brothers, K. N. Kudin, V. N. Staroverov, R. Kobayashi, J. Normand, K. Raghavachari, A. P. Rendell, J. C. Burant, S. S. Iyengar, J. Tomasi, M. Cossi, N. Rega, N. J. Millam, M. Klene, J. E. Knox, J. B. Cross, V. Bakken, C. Adamo, J. Jaramillo, R. Gomperts, R. E. Stratmann, O. Yazyev, A. J. Austin, R. Cammi, C. Pomelli, J. W. Ochterski, R. L. Martin, K. Morokuma, V. G. Zakrzewski, G. A. Voth, P. Salvador, J. J. Dannenberg, S. Dapprich, A. D. Daniels, Ö. Farkas, J. B. Foresman, J. V. Ortiz, J. Cioslowski and D. J. Fox, Gaussian Inc., Wallingford, CT, 2016.

43 A. D. Becke, *Phys. Rev. A*, 1988, **38**, 3098–3100.

44 C. T. Lee, W. T. Yang and R. G. Parr, *Phys. Rev. B: Condens. Matter*, 1988, **37**, 785–789.

45 B. Miehlich, A. Savin, H. Stoll and H. Preuss, *Chem. Phys. Lett.*, 1989, **157**, 200–206.

46 T. Yanai, D. P. Tew and N. C. Handy, *Chem. Phys. Lett.*, 2004, **393**, 51–57.

47 V. G. Zakrzewski, J. V. Ortiz, J. A. Nichols, D. Heryadi, D. L. Yeager and J. T. Golab, *Int. J. Quantum Chem.*, 1996, **60**, 29–36.

48 X. C. Pan, C. Fang, M. Fantin, N. Malhotra, W. Y. So, L. A. Peteanu, A. A. Isse, A. Gennaro, P. Liu and K. Matyjaszewskit, *J. Am. Chem. Soc.*, 2016, **138**, 2411–2425.